Scattering Matrix Method Applied to the Characterisation of Multilayered Porous Silicon Structures

Alexandre REINHARDT, Paul SNOW
Department of Physics, University of Bath, Bath, United Kingdom
Vincent LAUDE, Abdelkrim KHELIF, Sylvain BALLANDRAS,
Département LPMO, Institut FEMTO-ST, Besançon, France

Abstract. We describe a numerical model initially aimed at simulating the propagation of acoustic surface waves in multilayered structures and show how it can be used to the prediction of the electric response of a non-focusing ultrasonic transducer. We also apply this model to non-destructive evaluation of the elastic properties of porous silicon.

1. Introduction

A lot of effort has been devoted to the simulation of acoustic waves in multilayers. Simple one-dimensional models, like Mason's [1], are widely used to simulate acoustic transducers operating in piston-mode while neglecting the effects linked to the finite lateral dimensions of these devices [2]. On the other hand, models also focusing on the propagation in the lateral direction rather than in the thickness direction have appeared first due to works of geophysicists and then of researchers interested in Surface Acoustic Wave (SAW) devices. They allow the study of waves guided at the surface of a substrate or in a set of layers, like Lamb, Love or Stoneley waves. Such models have proven useful for example in the evaluation of concrete [3] or metallic structures for which corrosion induces a degradation of the surface, generating a layer exhibiting different acoustic properties from the main material. Being able to determine these changes and the thickness of this layer is crucial to diagnose the degradation of materials.

The case of porous silicon is very similar: the top part of a silicon wafer can be porosified over a depth of a few microns by electrochemical etching [4]. Although highly inhomogeneous, mesoporous type porous silicon etched in p-doped wafers, which is the only type of porous silicon we will consider in this paper, exhibits pores with a diameter in the order of a few tens of nanometres only, therefore much smaller than optical or acoustic wavelengths. This enables light or sound to propagate without experiencing a dramatic amount of scattering so that we can consider using effective medium approximations [5]. Since porous silicon is also a light emitting material [6], [7], a lot of research has focused on its optical applications, where it has proven to be very versatile [8], [9]. More recently, an interest for its acoustic properties has appeared [10], [11]. Because at the present time no theoretical model is able to explain its mechanical properties and because of the various pore morphologies that can be obtained simply by changing the etching conditions [12], there is a strong need for acoustically characterising this material.

Fahmy and Adler have proposed in 1973 a matrix formulation to model numerically the propagation of surface or bulk acoustic waves [13]. Although very versatile, it was based on a transfer matrix approach that could generate numerical instabilities when simulating the propagation of inhomogeneous waves in structures containing thick layers at high frequency. To overcome this problem, Pastureaud *et al.* proposed a scattering matrix method that is more stable [14]. Initially, these models only considered piezoelectric or dielectric media. We have extended the initial Fahmy-Adler formulation to the case of perfectly conducting solids and to perfect fluids [15] or even to Newtonian viscous fluids [16]. We have also adapted this model so that it can be used to calculate the electric response of thickness-mode resonators [17].

In this paper, we will demonstrate the application of this model to non-destructive characterisation of multilayered samples made of porous silicon. In a first part, we will review the principle of the Fahmy-Adler formulation and of the scattering matrix method. We will then show how it can be used to calculate the electric response of piezoelectrically driven devices, especially ultrasound transducers. This will allow us to describe an experimental setup for characterising porous silicon samples.

2. Scattering Matrix Method

For the sake of simplicity, we will only consider purely acoustic waves in this section. The aim of the scattering matrix method is to simulate waves in a multilayered structure similar to the one represented in Fig. 1. This method is based on a Fahmy-Adler formulation, existing both for viscous fluids and for solids.

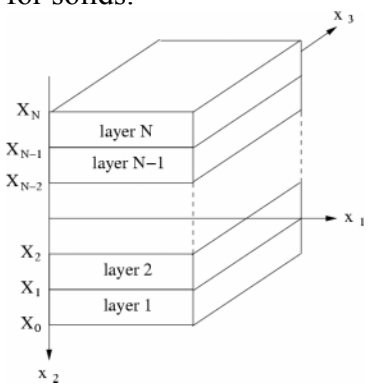

Fig. 1 – Axes and notation conventions used to represent a multilayer structure.

2.1. Fahmy/Adler Formulation

The original Fahmy-Adler formulation for a solid assumes the elastic properties and the density are that of a continuous and homogeneous medium. Assuming displacements or stress fields exhibit an harmonic time and space dependence with $\exp\left(j\omega(t-s_i x_i)\right)$, where $\boldsymbol{s}$ is the slowness vector, the problem of propagation of a plane wave in the medium can be expressed, as described in Ref. [15], as an eigenvalue problem involving the elastic tensor, the density and the projection of the slowness vector along the plane of the interfaces, which is constant for all layers according to Snell's law. The eigenvalues, that are found by pairs of complex conjugates or of opposite real values, provide the component of the slowness vector which is perpendicular to the interfaces, while the associated eigenvectors correspond to the polarisations of these plane waves. If we consider only purely elastic solids, the eigenvalue problem is of rank six. Thus, displacement and stress fields can be

written in the general way as a linear superposition of six plane waves, generally two longitudinal and four shear waves.

For Newtonian viscous fluids, a similar eigenvalue problem is found by using Stokes' law which relates shear stresses to deformations [18], [19], and by the use of the compressibility of the medium, which is the analogous of elasticity in a fluid. Here again, as demonstrated in Ref. [16], the dimension of the eigenvalue problem is six, resulting in six partial waves, corresponding to two longitudinal waves and four evanescent shear waves, that exhibit a very fast decay during their propagation in the vertical direction.

2.2. Scattering Matrix Method

To avoid any numerical instability at high frequency for thick layers, partial modes are assessed as "transmitted" or "reflected", depending on the direction of their Poynting vector for propagating partial modes, or on the direction in which they are evanescent in the case of partial modes whose s_2 slownesses exhibit an imaginary part. It is then convenient to introduce a reflection matrix relating the amplitudes of "reflected" partial waves to the amplitudes of the "incident" ones [14].

The first step in the scattering matrix method is to express the boundary conditions applied to the bottom side of the simulated structure. In practice, three cases are to be considered:

- A *semi-infinite medium*: this is the easiest case to deal with, as we can consider that no partial wave is reflected from any bottom surface. Therefore the reflection matrix in this medium is zero at all positions within the semi-infinite medium.
- A *stress free surface*, considered bounded by a vacuum. Waves are totally reflected, but with some possible mode couplings at the interface. To determine these couplings, we write that the stress fields cancel, what provides directly an expression for the reflection matrix [15].
- A *clamped surface*, considered bounded by an infinitely rigid medium. In a similar way, writing that the displacement fields cancel provides directly an expression for the reflection matrix and for mode conversions at the bottom surface [20].

Once the calculation of the reflection matrices has been initialized, we have to transfer this matrix iteratively from one layer to another in order to transfer the influence of the bottom boundary conditions and the overall mechanical behaviour of the structure to the top surface. At each interface, mode conversions can occur. This is determined by stating that displacement and stress fields are continuous across the interface between two media. Using these continuity relations, and knowing the reflection matrix in one layer, we can calculate the reflection matrix in the adjacent one.

We apply now these calculations to a structure made of a porous silicon slab atop a silicon substrate. For calculations, since there does not yet exist a model that provides the acoustic properties of porous silicon as a function of porosity, we use the results of measurements performed so far by acoustic microscopy and by Brillouin spectroscopy [10], [11]. We consider a 5 μm thick layer with a porosity of 50 %, meaning that it is made of air and silicon with equal volume fraction. This is approximately the kind of thicknesses that can be etched with a fairly uniform porosity. The silicon substrate is considered semi-infinite, what is a good approximation of a silicon wafer with an unpolished bottom surface. Finally, we consider the sample immersed in water, which is used as a coupling medium. Because of the hydrophobic behaviour of freshly etched porous silicon, we can consider that pores remain filled with air [10]. The fact that characterisations in air by optical means and in water by direct acoustic measurements come to an agreement validates this assumption [11]. Numerical values of material properties used in these calculations are summarized in Table 1.

Table 1 – Relevant material constants used for calculations. Quality factors (Q) and dielectric losses are given at a frequency of about 1 GHz.

Silicon	Porous silicon 50 % porosity	Water	ZnO
Cubic symmetry Density: 2330 kg/m^3 Elastic constants: c_{11} = 166 GPa, c_{44} = 79.6 GPa Mechanical losses: Q_m = 10000	Isotropic Density: 1165 kg/m^3 Elastic constants: c_{11} = 18.49 GPa, c_{44} = 8.83 GPa Mechanical losses: Q_m = 1000	Isotropic Density: 1000 kg/m^3 Compressibility: χ = 0.44 GPa-1 Shear viscosity: η = 0.8 cP Longitudinal viscosity: ζ = 2.24 cP	Hexagonal symmetry Density: 6346 kg/m^3 Elastic constants: c_{33} = 180.2 GPa Mechanical losses: Qm = 2000 Piezoelectric constants: e_{33} = 1.28 C/m^2 Dielectric constants: $\varepsilon_{33} = 10.5.10^{-11}$ F/m Dielectric losses: tan $\delta = 10^{-4}$

The reflection coefficient in water of a longitudinal wave at normal incidence is shown Fig. 2. To illustrate the attenuation of water at GHz frequencies, that cause the amplitude of waves propagating in the liquid to reduce with distance, thus reducing the effective modulus of the reflection coefficient, we have calculated this reflection coefficient on virtual planes positioned at several distances from the surface of the structure. As can be seen, the effect of viscosity is frequency dependent and tends to decrease the contrast of the acoustic fringes, causing them to be difficult to measure at a distance of more than about 30 µm.

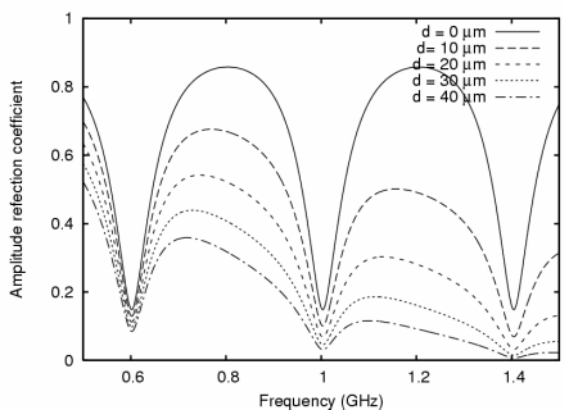

Fig. 2 – Amplitude reflection coefficient of a longitudinal wave in water at normal incidence over a 5 µm porous silicon (with 50 % porosity) slab atop a semi-infinite silicon substrate. This reflection coefficient has been evaluated at several distances *d* from the surface of the structure.

2.3. Green's Functions

Green's functions are a useful concept used to represent numerically the response to applied stresses of a medium or of a stratified structure. In practice, they are defined as the linear relationship relating displacements of a surface to the applied stresses. Because both displacements and stresses at the top surface of the structure can be expressed as a function of the properties of the partial waves in the upper layer and of the reflection matrix on the top surface, Green's functions are calculated using these two characteristics, as shown in Ref. [14].

One of the applications of these functions is the characterisation of acoustic modes existing in a multilayered structure. Dispersion curves can be obtained by looking at the zeroes of the determinant of the inverse of the Green's functions [21]. In Fig. 3, we have simply represented in grey scale the amplitudes of the normal displacements (u_2) as a

function of the normal stress or pressure applied to the structure (T_{22}). Acoustic modes are represented by the generation of relatively large displacements (dark lines).

Fig. 3(a) shows the acoustic modes of the porous silicon slab atop a semi-infinite substrate studied in the previous subsection. For low wave vectors (left side), generated modes are leaky because they radiate power within the substrate, hence their lighter color. Once the critical angle between porous silicon and silicon is reached (high wave vectors, or right side), modes are trapped within the porous layer and therefore generate larger displacements at the top of the structure, causing lines to appear darker on the plot [22]. These correspond to Love waves or to generalised Lamb waves, depending on their polarisations. Fig. 3(b) has been calculated using the same structure covered by 15 µm of water. When a coupling from a mode of the water layer to a mode of the solid structure occurs, branches appear leaky on this figure. This is how some of the modes of the structure can be detected by a non-contact measurement.

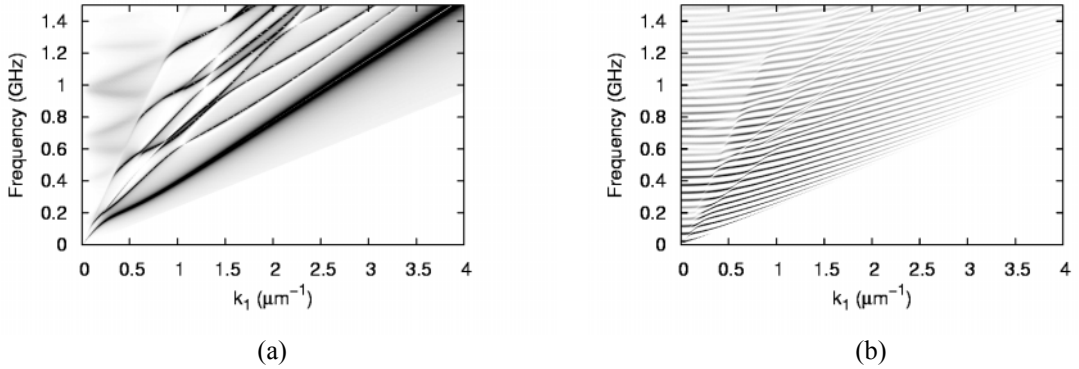

(a) (b)

Fig. 3 – G_{22} component of the Green's functions plotted as a function of lateral wave vector (k_1) and frequency and represented in grey scale (arbitrary units), (a) for a 5 µm porous silicon (50 % porosity) atop a semi-infinite silicon substrate and (b) for the same structure covered by 15 µm of water.

3. Calculation of Electric Responses

In the previous section, we have only considered the physical behaviour of a multilayered structure and its interactions with the surrounding medium. We will now consider ultrasonic transducers which are used to generate acoustic waves and at the same time to detect them. This is necessary to consider the interactions between the transducer and the structure being measured.

3.1. Electromechanical Behaviour of a Multilayered Structure

In section 2.1 we only considered purely mechanical effects. However, the Fahmy-Adler formulation has been established to represent acoustic waves in piezoelectric media [13]. Therefore, it is based on the linear equations of piezoelectricity that include also the electric field and the electric displacement and relating them to the mechanical displacements and stresses via the piezoelectric coefficients [23]. However, calculations remain formally the same in the frame of the quasistatic approximation, excepted that the dimension of the eigenvalue problem is now eight instead of six.

Dielectric materials, either fluids or solids, can be considered in the same way, although the electrostatic and mechanical problems are decoupled. We can therefore calculate the partial waves in the medium in the usual way, and determine separately the electrostatic partial modes, for which analytic expressions exists.

We consider finally that conducting materials, like metals or fluids like water, for example, are perfectly conducting. Therefore, the electric potential is supposed a constant in the medium. To remain compatible with the assumption of waves having a lateral propagation, and thus with the hypothesis of a spatially varying electric potential, we suppose that the medium is grounded. This causes also the electric displacement to vanish, but the latter can be discontinuous across an interface if a surface charge density exists. These two assumptions provide an additional equation to the three mechanical ones when considering the continuity of fields between two media, and therefore equilibrate the problem of determining mode conversions at an interface [15].

The only location where we allow a conducting medium not to be grounded is when it is located at the topmost layer of a structure. There, a non-zero electric potential can be considered as a boundary condition. Since the electrostatic behaviour of the structure is also contained within the reflection matrices, the Green's functions calculated as in subsection 2.3 also includes the electric response of the simulated structure. Once the surface charge density at the top of the structure is known, the electric admittance is then defined as $Y = I/V$.

Falling back to our example, we will now focus on the simulation of an acoustic transducer to be used to measure the porous silicon/silicon structure studied previously. We have calculated in Fig. 4 the theoretical response of an acoustic transducer made of a thin (2.5 µm) Zinc Oxide (ZnO) film atop a 500-µm-silicon buffer. This buffer is also coated with two impedance matching layers (two quarter-wavelengths of theoretical materials having acoustic impedances respectively equal to $Z_1 = Z_{si}^{2/3}.Z_{water}^{1/3}$ and $Z_2 = Z_{si}^{1/3}.Z_{water}^{2/3}$). Despite these matching layers, reflections of longitudinal waves between the silicon buffer and water still occur, as the impedance contrast between each of these layers is still very large.

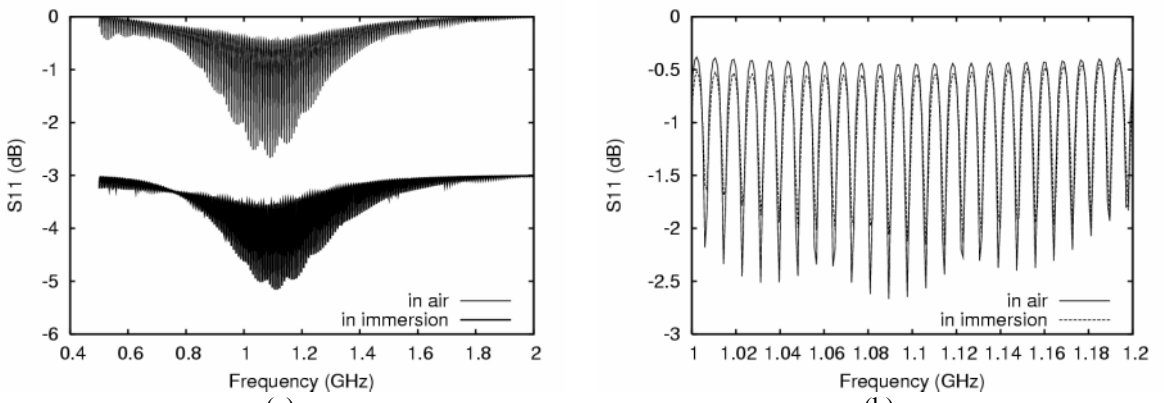

Fig. 4 – Theoretical response of an ultrasonic transducer made of a thin ZnO film atop a silicon substrate, coated with two impedance matching layers: (a) broad band spectrum both in air and in water (note that the response of the transducer in water has been shifted by –3 dB for legibility), (b) part of the spectrum only, demonstrating the influence of water on the electric response.

In Fig. 5, we have calculated the electric reflection spectra for a structure made of the transducer simulated previously, a thin layer of water, and then the porous silicon slab atop a semi infinite silicon wafer that has been studied in section 2. These calculations have been performed for several water thicknesses in order to show the influence of the coupling medium in this configuration. Some fringes are visible for low thicknesses, corresponding to the standing waves in the water film that are visible in Fig. 3 and Fig. 4. They remain as long as the thickness of water is sufficiently low for attenuation no to prevent standing waves to be established. Nevertheless, fringes due to the reflection spectrum of the solid structure are difficult to distinguish among them, as expected from Fig. 3.

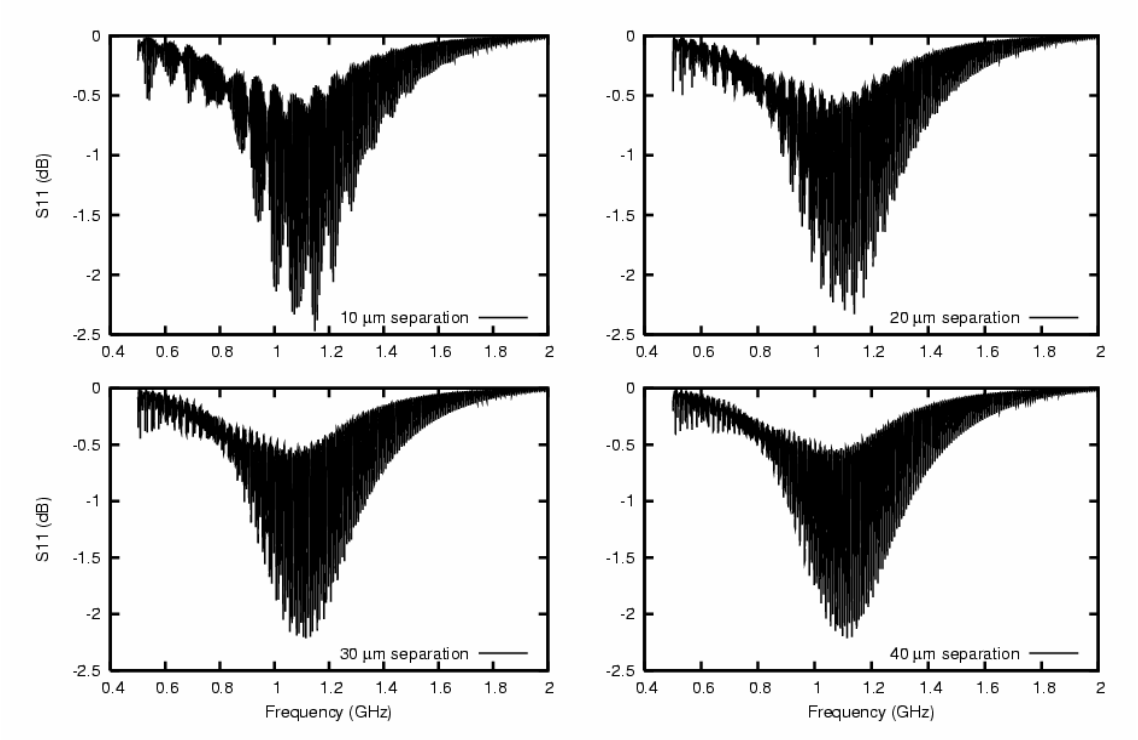

Fig. 5 – Theoretical electric reflection spectra for the transducer simulated in Fig. 4 used to measure the porous silicon structure studied in section 2, for several separation distances.

3.2. Time Domain Analysis

A classical technique to evaluate directly the ratio thickness/velocity is to perform measurements in the time domain, where each reflection is identified by an estimation of the time of flight of acoustic pulses, rather than in the frequency domain. By calculating the Fourier transform of the admittance curves, current forms as shown in Fig. 6 are obtained. On subfigure (a), the comparison between the time-domain response of the transducer radiating in water alone and the one with the transducer illuminating the sample reveals that most of the echoes are generated inside the transducer, especially the ones at 120 and 240 ns that correspond to the reflection of waves at the end of the silicon buffer and of the impedance matching layers. Between these two echoes, a smaller one corresponds to reflections at the two surfaces limiting the porous silicon slab, as the acoustic impedance

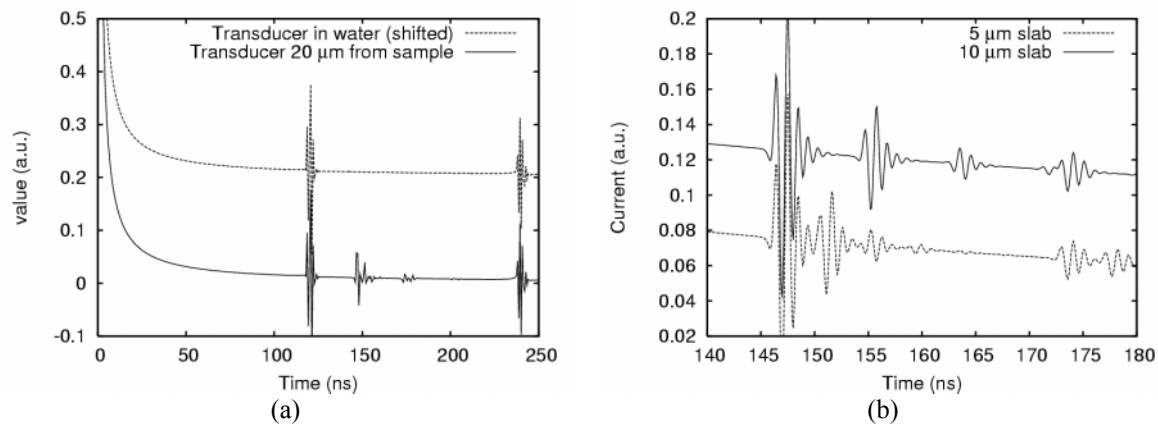

Fig. 6 – Time domain transformation of the calculated signal (a) and zoom around the two pulses due to the sample structure (b).

contrast is lower.

Fig. 6(b) provides a more detailed view of the pulses. Since the transducer has a finite bandwidth, spectral broadening of the pulse (here supposed to be a quasi-Dirac function) occurs. For this reason, a few oscillations are visible at the time at which the echo on the top surface of the sample occurs, thus causing a mixing with the echo corresponding to the interface between silicon and porous silicon. To demonstrate this effect, we have also added to calculation obtained for a 10 µm-thick porous silicon slab. In this case, echoes on the top surface (at 147 ns) and on the bottom surface (at 155 ns) of the slab are well defined.

4. Conclusion

In this paper, we have given a broad overview of the scattering matrix method and applied it to the characterisation of porous silicon samples, for which we have calculated reflection spectra, the localisation of acoustic fields, and dispersion curves. This has given some insight into the ways in which we can characterise them. In a second part, we have focused on the design of an ultrasonic reflection experiment, by considering the interactions between an ultrasonic transducer operating at very high frequency and the studied sample.

Acknowledgements

The work performed for developing the numerical model was sponsored by Temex, Sophia Antipolis, France. Work on porous silicon was funded by the UK Engineering and Physical Science Research Council.

References

[1] W. P. Mason, *Phys. Rev.* **55**, 775 (1939).
[2] A. Ballato, *IEEE Trans. on Ultrason., Ferroelec. and Freq. Contr.* **48**, 1189 (2001).
[3] M. Goueygou *et al.*, *Proceedings of the 2001 IEEE Ultrasonics Symposium*, 761 (2001).
[4] R.L. Smith and S.D. Collins, *J. Appl. Phys.* **71**, R1 (1992).
[5] W. Theiβ, *Surface Science Reports* **29**, 91 (1997).
[6] L.T. Canham, *Appl. Phys. Lett.* **57**, 1046 (1990).
[7] A. Halimaoui *et al.*, *Appl. Phys. Lett.* **59**, 304 (1991).
[8] M. G. Berger *et al.*, *Thin Solid Films* **297**, 137 (1997).
[9] L.Pavesi, *Riv. Nuovo Cimento* **20**, 1 (1997).
[10] R.J.M. DaFonseca *et al.*, *Superlattices and Microstructures* **16**,21 (1994).
[11] H.J. Fan *et al.*, *Phys. Rev. B* **65**, 165330 (2002).
[12] A.M. Polomska *et al.*, *Porous Silicon Science and Technology 2006 Proceedings*, paper 06-06 (2006).
[13] A. H. Fahmy, E. L. Adler, *Appl. Phys. Lett.* **22**, 495 (1973).
[14] T. Pastureaud, V. Laude, S. Ballandras, *Appl. Phys. Lett*. **80**, 2544 (2002).
[15] A. Reinhardt, T. Pastureaud, S. Ballandras, V. Laude, *J. Appl. Phys*. **94**, 6923 (2003).
[16] S. Ballandras *et al.*, *J. Appl. Phys*. **99**, 054907 (2006).
[17] A. Reinhardt *et al.*, *Proceedings of the 2002 IEEE Ultrasonics Symposium*, 480 (2002).
[18] J. Kestin, R. Dipippo, *American Institute of Physics Handbook*, Chapter 2. Mc Graw-Hill, 3rd Edition.
[19] W.P. Mason editor, *Physical Acoustics, Principle and Methods*, vol. IA, Chapter 1, pp. 1-110. Academic Press, New York, San Francisco, London, 1964.
[20] A. Reinhardt *et al.*, *IEEE Trans. Ultrason., Ferroelec. And Freq. Contr.* **51**, 1157 (2004).
[21] L. Dobrzynski *et al.*, *Phys. Rev. B*, **35**, 5872 (1987).
[22] B.A. Auld, *Acoustic fields and waves in solids* vol. 2, Krieger publishing, Malabar, Florida (1990).
[23] ANSI/IEEE Std 176-1987, IEEE Standard on piezoelectricity (1987).